Supplementary Material for "Microscopic Reversibility and Emergent Elasticity in Ultrastable Granular Systems"

1 CALCULATION OF $C_{ijkl}(\theta)$ IN THE LONG-WAVELENGTH LIMIT

1.1 The rotated reference frame $x'y'$

As mentioned in the main text, we find that it is most convenient to examine the stress correlations in a frame $x'y'$ that is rotated by $\pi/4$ clock-wisely from the original xy frame. We express everything in this rotated frame. We show in Fig. S1(a) a polarized image in the $x'y'$ frame. The axes for the original xy directions are also plotted.

1.2 Construct stress fields

Following the procedure detailed in Ref. Nampoothiri et al. (2020), we first define a particle-scale stress tensor for each individual disc. For the gth disc, we define

$$\hat{\sigma}_g = \frac{1}{A_g} \sum_{k=1}^{z_g} \mathbf{r}_k \otimes \mathbf{f}_k, \tag{S1}$$

where A_g is the Voronoi area for the gth particle, $\mathbf{r}_k$ and $\mathbf{f}_k$ are the branch vector and contact force vector corrspond to the kth contact, and the summation of k goes over all contacts on the gth particle.

To construct a stress field σ_{ij}, where i and j can be either x' or y', we let $\sigma_{ij}(x', y') = \hat{\sigma}_{g,ij}$ if (x, y) belongs to the Voronoi cell of particle g. Figure S1(b) shows the constructed $\sigma_{y'y'}$ field for the state shown in Fig. S1(a).

1.3 Calculate the Fourier transformation of stress fields

To avoid complications introduced from the system boundaries, we consider three square regions of interest (ROIs) as shown in Fig. S1(b). Each ROI has a side length $L = 16d_\mathrm{s}$ where d_s is the diameter of the smaller disc.

For each ROI stress field σ_{ij}, we first calculate the deviation from the mean

$$\delta\sigma_{ij}(x', y') = \sigma_{ij}(x', y') - \langle\sigma_{ij}\rangle, \tag{S2}$$

where $\langle\cdot\rangle$ represent a spatial average. We then calculate the Fourier transform of $\delta\sigma_{i'j'}$ as following

$$\widetilde{\delta\sigma}_{ij}(\mathbf{q}) = \frac{1}{2\pi} \int \delta\sigma_{ij}(\mathbf{r}) e^{-i\mathbf{q}\cdot\mathbf{r}} d\mathbf{r} \tag{S3}$$

In practice, we perform the discrete Fourier transformation

$$\widetilde{\delta\sigma}_{ij}(q_{x'}, q_{y'}) = \frac{1}{2\pi} \sum_{n=1}^{N} \sum_{m=1}^{N} \delta\sigma_{ij}(n\Delta x', m\Delta y') e^{-iq_{x'}n\Delta x'} e^{-iq_{y'}m\Delta y'} \Delta x' \Delta y', \tag{S4}$$

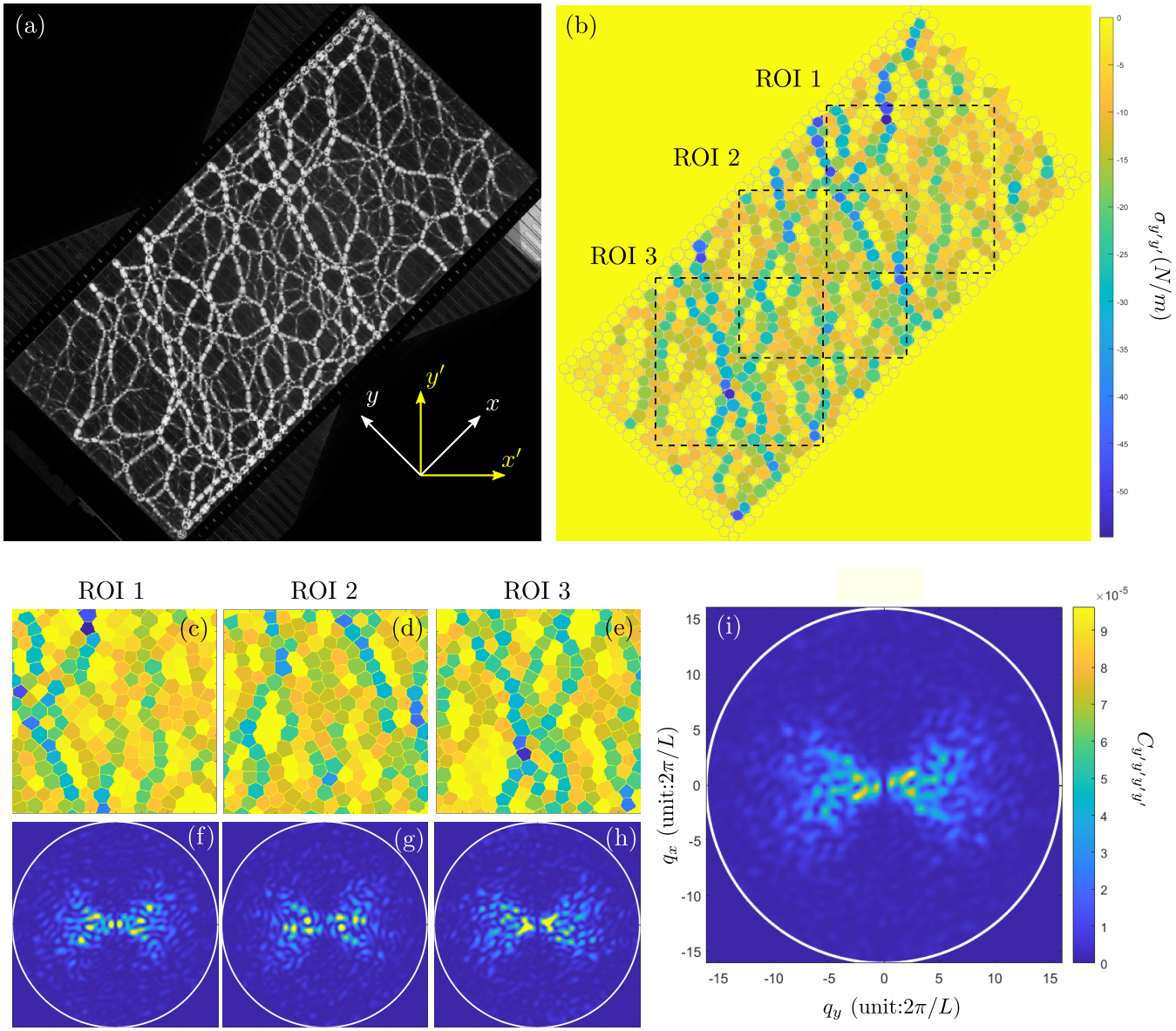

Figure S1. (a) The plolarized image for an example ultrastable state formed by $\gamma_{\mathrm{I}} = 0.147$ and $\delta\gamma = 0.95\%$. The direction of axes are sketched. (b) The continuous stress field $\sigma_{y'y'}$ constructed from the particle-scale stress tensors for the state shown in (a). The three regions of interest (ROI) are sketched. (c-e) shows zoom-in versions of the three ROIs in (b). (f-g) shows the correlation functions $C_{y'y'y'y'}$ calculated from the stress fields in (c-e) respectively. (i) The correlation function for the state in (a) obtained by averaging the correlation functions shown in (f-g). The color scales in (c-e) are the same as in (b). The color scales in (f-h) are the same as in (i). Note that $L = 16d_{\mathrm{s}}$ where d_{s} is the diameter of the smaller disc. L is the side length of the square ROIs.

where $\Delta x' = \Delta y' = td_{\mathrm{s}}/2$ and $t = 0.81$ is a constant. We have tested that using a smaller t gives similar results. $N\Delta x' = N\Delta y' = L$ that is the side length of the ROIs.

1.4 Calculate the Fourier transform of the correlation functions

The stress correlation functions in the Fourier space for a certain packing is calculated by

$$C_{ijkl}(\mathbf{q}) = C_{ijkl}(q_{x'}, q_{y'}) = \widetilde{\delta\sigma}_{ij}(q_{x'}, q_{y'})\widetilde{\delta\sigma}_{kl}(-q_{x'}, -q_{y'}). \tag{S5}$$

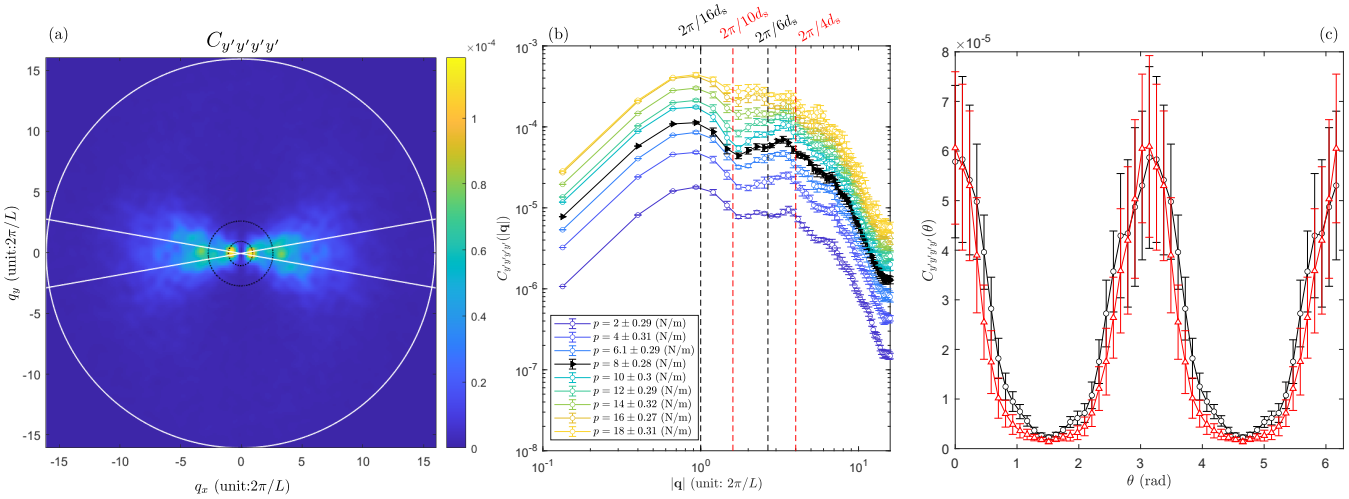

Figure S2. (a) The ensemble-averaged correlation function $C_{y'y'y'y'}(\mathbf{q})$ from 30 original shear-jammed states with averaged pressure $p = 8 \pm 0.28$ N/m. The two black dotted circles have radii $2\pi/16d_s$ and $2\pi/6d_s$. The two white lines form an angle $\pi/9$, within which the radial functions $C_{y'y'y'y'}(|\mathbf{q}|)$ shown in (b) are calculated. (b) The radial dependence of the correlation functions for ensembles of original shear-jammed states with different stress states. The black curve corresponds to the function shown in (a). (c) The angular function $C_{y'y'y'y'}(\theta)$ for the same ensemble shown in (a) calculated by averaging radial parts within the regime between the two black dashed lines in (b) (black circles) and within the regime between the two red dashed lines in (b) (red triangles).

For each packing, we first calculate C_{ijkl} for the three ROIs, and the stress-stress correlation function C_{ijkl} for this state is obtained by averaging over the three ROIs. Figure S1(f-h) plots the calculated $C_{y'y'y'y'}$ for the three ROIs as shown in (c-e), while the final result is shown in (i) which is obtained by averaging the three functions shown in (f-h).

1.5 Calculate the ensemble averaged correlation functions

After obtaining the correlation function $C_{ijkl}(\mathbf{q})$ for all states. We calculate the ensemble-averaged correlation functions for states with similar stress states. The final result is

$$C_{ijkl}(\mathbf{q}) = \langle C_{ijkl}(\mathbf{q}) \rangle, \tag{S6}$$

where $\langle \cdot \rangle$ represents ensemble average. In the main text, we always consider the ensemble-averaged correlation functions. Figure S2(a) plots the ensemble averaged correlation function $C_{y'y'y'y'}$ over 30 different packings of original shear-jammed states, which appears more smooth than correlation functions obtained from individual packings such as the one shown in Fig. S1(i).

1.6 Identify the continuum limit using the radial dependence of the correlation functions

The Vector Charge Theory of Granular Mechanics (VCTG) Nampoothiri et al. (2020, 2022) predicts features of the correlation functions in the long-wavelength limit ($|\mathbf{q}| \to 0$). To compare to the theory, we need to identify the range of $|\mathbf{q}|$ where the system can be regarded to be in the long-wavelength limit. Thus, we examine the radial dependence of the correlation functions in our systems and focus on the regime where C_{ijkl} does not depend on $|\mathbf{q}|$.

As examples, we consider ensembles of original shear-jammed states. We plot $C_{y'y'y'y'}(|\mathbf{q}|)$ along $\theta = \pi$ direction in Fig. S2(b) for ensembles with different stress states. In practice, these curves are averaged

from angular direction $\theta \in (\pi - \pi/18, \pi + \pi/18)$. The black triangle curve corresponds to the correlation function shown in (a). The data with $|\mathbf{q}| < 2\pi/L$ is not of our interest. All $C(\theta)$ data shown in the main text are obtained by averaging over $|\mathbf{q}|$ between $2\pi/16d_{\mathrm{s}}$ and $2\pi/6d_{\mathrm{s}}$, as marked by the two black dashed lines in Fig. S2(b). In this regime, $C_{y'y'y'y'}$ roughly display a plateau expect perhaps near the system size ($|\mathbf{q}| \approx 2\pi/16d_{\mathrm{s}}$) where it shows a clear growth. A similar feature was carefully examined in Ref. Lemaître et al. (2021) and was attribute to the history-dependent nature of frictional contact forces. The plateau is perhaps better defined in the regime between $2\pi/10d_{\mathrm{s}}$ and $2\pi/4d_{\mathrm{s}}$ as marked by the two red dashed lines in Fig. S2(b). We find that averaging in the regime between the two black dashed lines or between the two red dashed lines do not lead to drastically different angular functions $C_{y'y'y'y'}(\theta)$. For example, the black and red curve in Fig. S2(c) are correlation functions for same ensemble as shown in (a) whose radial parts are averaged in the regime between the two black dashed lines and in the regime between the two red dashed lines respectively. It appears that the angular dependence of the two curves remain almost the same.

1.7 Calculate the angular dependence of the cross-correlation functions

After identifying the range of $|\mathbf{q}|$ where $C(\mathbf{q})$ displays a plateau, we calculate the angular functions $C(\theta)$ by averaging the radial parts in the plateau regime. In the main text, all $C(\theta)$ curves are calculated by averaging the radial parts in the regime between the two black dashed lines in Fig. S2(b).

REFERENCES

Lemaître, A., Mondal, C., Procaccia, I., Roy, S., Wang, Y., and Zhang, J. (2021). Frictional granular matter: Protocol dependence of mechanical properties. *Phys. Rev. Lett.* 126, 075501. doi:10.1103/PhysRevLett.126.075501

Nampoothiri, J. N., D'Eon, M., Ramola, K., Chakraborty, B., and Bhattacharjee, S. (2022). Tensor electromagnetism and emergent elasticity in jammed solids. *arXiv preprint arXiv:2204.11811*

Nampoothiri, J. N., Wang, Y., Ramola, K., Zhang, J., Bhattacharjee, S., and Chakraborty, B. (2020). Emergent elasticity in amorphous solids. *Phys. Rev. Lett.* 125, 118002. doi:10.1103/PhysRevLett.125.118002